The 5th Joint International Conference on Multibody System Dynamics
June 24 – 28, 2018, Lisboa, Portugal

Acceleration-based strain estimation in a beam-like structure

Johannes Luthe[1], Andreas Schulze[1], Roman Rachholz[1], János Zierath[2] and Christoph Woernle[1]

[1] *Chair of Technical Dynamics, University of Rostock, 18051 Rostock, Germany, {johannes.luthe, andreas.schulze2, roman.rachholz, woernle}@uni-rostock.de*
[2] *W2E Wind to Energy GmbH, 18055 Rostock, Germany, jzierath@wind-to-energy.de*

ABSTRACT — *Measuring and logging of fatigue loads is essential for individual life time estimations of operating wind turbines. This contribution investigates the quality of the widely accepted modal decomposition and expansion (MDE) approach for the estimation of fatigue indicators on the basis of a limited number of acceleration measurements. A cantilever beam is chosen as simple test structure in order to identify possible pitfalls inherent to the MDE method in a transparent way. Analytical mode shapes are chosen as basis for the modal expansion as a first approach. Several experimental tests approve the feasibility of this procedure and show good agreement between measured and estimated fatigue indicators after minor model refinements based on experimental modal analysis. Future investigations include the application of this method to full-scale wind turbines.*

1 Introduction

The global challenge of limited fossil resources causes a growing significance of renewable energies. Due to their comparatively high energy efficiency wind turbines play an important role to accomplish the transition to sustainable energy sources. A robust design of the mechanical components of wind turbines with respect to fatigue behaviour is a prior target in the dimensioning process. According to the certification guidelines by DNV GL [1] wind turbines are designed for a life time of at least 20 years. However, the design load assumptions are conservative compared to the actual loads acting on a physical wind turbine, implying a discrepancy between the actual and anticipated fatigue progression. Thus, in order to asses the individual life time of a wind turbine, reliable tracking of the actually endured fatigue loads at critical spots is of great interest. Direct measurement of strains in operating wind turbines imposes high requirements on the measurement equipment and is in any case only possible at accessible measurement positions. An indirect derivation of fatigue indicators by rather simply obtainable motion quantities, e.g. accelerations, is more reasonable in this context.

The aim of this contribution is to provide a basis for the fatigue estimation based on a limited number of acceleration measurements applying the Modal Decomposition and Expansion (MDE) approach. The MDE is a widely accepted method for full-field stress and strain recovery and has been applied on a wide range of mechanical and civil structures [2–5]. A comparison with other state-of-the-art strain estimation methods like Kalman filtering and joint-input filtering techniques is given in [6]. Despite the already existing application cases, the goal of this contribution is to identify possible pitfalls which are connected with the practical implementation of the MDE in a separate simple testing environment. This is reasonable since practical investigations on physical wind turbines always require standstill periods and must therefore be reduced to a minimum.

On that account, first practical tests were conducted on a steel cantilever beam which can be regarded as simplified model of a wind turbine tower. The experiences made are considered as basis for future applications on a small scale wind turbine [7] as well as on a full scale prototype turbine [8].

The paper is organised as follows. Section 2 briefly describes the basic principle of the MDE and the required signal processing. Furthermore an outlook to fatigue estimation methods is given. In Sec. 3 the introduced procedure is investigated in practical tests, and results are discussed in detail. In addition, a model refinement is performed on the basis of experimental modal analysis.

2 Theoretical background

In Sec. 2.1 the basic principle of modal decomposition and expansion is illustrated. As an overview, the required steps for the computation of strain estimations on the basis of MDE are depicted in Fig. 2. The necessary signal processing is explained in Sec. 2.2. Basic fatigue estimation methods are introduced in Sec. 2.3.

2.1 Modal decomposition and expansion

In general, the dynamic displacement $w(x,t)$ of a continuous one-dimensional system can be represented by the linear combination of its continuous mode shapes $\varphi_j(x)$ and modal coordinates $q_j(t)$ with $j = 1,\dots,\infty$. In practice, depending on the frequency range of excitation, usually only a small set of n lower modes provide a significant contribution to the dynamic displacement. Thus, the omission of higher modes (modal truncation) allows for the approximation of $w(x,t)$ by a finite sum,

$$w(x,t) = \sum_{j=1}^{\infty} \varphi_j(x)\, q_j(t) \approx \sum_{j=1}^{n} \varphi_j(x)\, q_j(t)\,. \tag{1}$$

In the application case of a wind turbine tower the first three bending modes can be identified as most significant [8], thus $n = 3$.

Relation (1) is exploited for the principle of MDE on a given set of vibration measurements. Due to their reliability and robustness accelerometers are usually used in the field of structural dynamics. The measured accelerations conducted at discrete positions x_k, $k = 1,\dots,m$ are combined into the vector $\ddot{\boldsymbol{w}}(t) \in \mathbb{R}^m$,

$$\ddot{\boldsymbol{w}}(t) = \begin{bmatrix} \ddot{w}(x_1,t) & \dots & \ddot{w}(x_m,t) \end{bmatrix}^{\mathrm{T}} \tag{2}$$

For modal decomposition of $\ddot{\boldsymbol{w}}(t)$ n continuous shape functions $\varphi_j(x)$, each evaluated at the m measurement positions x_k, and n modal accelerations $\ddot{q}_j(t)$ are required which can be combined into the vectors $\boldsymbol{\phi}_j \in \mathbb{R}^m$ and $\ddot{\boldsymbol{q}}(t) \in \mathbb{R}^n$, respectively,

$$\boldsymbol{\phi}_j = \begin{bmatrix} \varphi_j(x_1) & \dots & \varphi_j(x_m) \end{bmatrix}^{\mathrm{T}}, \quad j = 1,\dots,n \tag{3}$$

and

$$\ddot{\boldsymbol{q}}(t) = \begin{bmatrix} \ddot{q}_1(t) & \dots & \ddot{q}_n(t) \end{bmatrix}^{\mathrm{T}}. \tag{4}$$

With Eq. (3) and (4) the set of acceleration measurements $\ddot{\boldsymbol{w}}(t)$ can be approximately modally decomposed according to Eq. (1),

$$\ddot{\boldsymbol{w}}(t) \approx \underbrace{\begin{bmatrix} \boldsymbol{\phi}_1 & \dots & \boldsymbol{\phi}_n \end{bmatrix}}_{\boldsymbol{\Phi}} \ddot{\boldsymbol{q}}(t)\,. \tag{5}$$

The mode shape matrix $\boldsymbol{\Phi} \in \mathbb{R}^{m \times n}$ includes the n mode shape vectors $\boldsymbol{\phi}_j$. If n matches m, i.e. the number of measurement location equals the number of modes of interest, a direct approximation $\ddot{\tilde{\boldsymbol{q}}}(t)$ for the modal accelerations can be obtained,

$$\ddot{\boldsymbol{q}}(t) \approx \ddot{\tilde{\boldsymbol{q}}}(t) = \boldsymbol{\Phi}^{-1}\, \ddot{\boldsymbol{w}}(t)\,. \tag{6}$$

In case more measurements than modes of interest are available, a least-squares solution can be found for $\ddot{\tilde{\boldsymbol{q}}}(t)$.

The mode shapes matrix $\boldsymbol{\Phi}$ is to be derived either by experimental modal analysis [9], finite element (FE), multibody [10, 11] or idealised analytical models. All these approaches assume that the experimental or numerical mode shapes correspond sufficiently to their physical counterparts. In the context of this contribution analytical mode shapes are chosen as a first approximation as exemplary shown in Fig. 1.

To find an analytical approximation for the axial strain field $\varepsilon_x(x,z,t)$ at any location x,z in the beam structure, the EULER-BERNOULLI theory is exploited according to which the axial strains are directly linked to the beam curvature

$$\varepsilon_x(x,z,t) = -w''(x,t)\,z\,, \tag{7}$$

with z being the distance to the neutral axis.

With reasonable estimations for the modal accelerations $\ddot{\bar{\boldsymbol{q}}}(t)$ from Eq. (6) the beam curvature acceleration $\ddot{w}''(x^*,t)$ at any location x^* can be approximated by means of modal expansion according to relation (1),

$$\ddot{w}''(x^*,t) \approx \ddot{\bar{w}}''(x^*,t) = \sum_{j=1}^{n} \varphi_j''(x^*)\,\ddot{q}_j(t)\,, \tag{8}$$

with $\varphi_j''(x^*),\ j = 1,\ldots,n$ being the n curvature or strain mode shapes, respectively, evaluated at location x^*.

Note that $\varphi_j''(x)$ can be directly expressed in closed form when considering the analytical mode shapes, Fig. 1c. In contrast to that, FE or multibody models provide curvature mode shapes only in terms of discrete vectors at the respective node locations. For the modal expansion to position x^* an appropriate interpolation of the curvature mode shape vectors is required in general.

Combining Eq. (7) and Eq. (8) eventually yields an estimation for uni-axial strains $\bar{\varepsilon}_x(x^*,z,t)$,

$$\varepsilon_x(x^*,z,t) \approx \bar{\varepsilon}_x(x^*,z,t) = -z\,\bar{w}''(x^*,t). \tag{9}$$

Equation (9), however, requires a twofold time integration of the curvature acceleration $\ddot{\bar{w}}''(x^*,t)$, which has to be performed with special care, see Sec. 2.2 for further details.

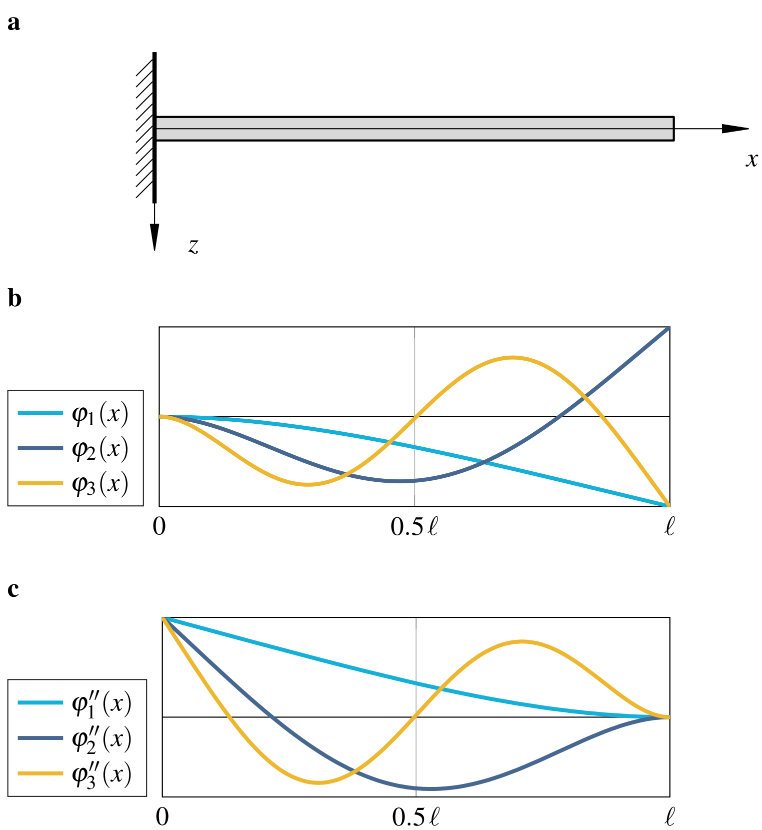

Fig. 1: **a** Cantilever beam model of length ℓ **b** The first $n = 3$ uni-axial bending mode shapes **c** The corresponding strain mode shapes.

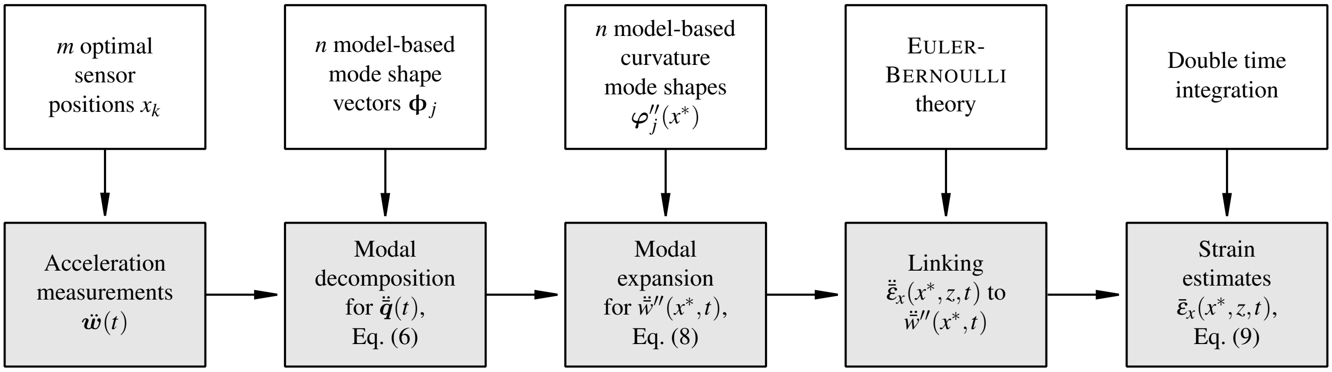

Fig. 2: Required steps for strain estimations on the basis of MDE

2.2 Signal processing

In general, the integration of discrete time signals is a common signal processing task. An overview of different methods, among them both time and frequency domain techniques, is given in [12]. In addition, different well-established integration methods are investigated in detail concerning their relative integration error in [13]. It is shown that intuitive integration in frequency domain – i.e. performing a Discrete Fourier Transform (DFT) of the time signal, dividing the spectrum by $\mathrm{i}\omega$ followed by inverse DFT – is superior to all other analysed techniques. On that account, the curvature acceleration $\ddot{\bar{w}}''(x^*,t)$, Eq. (7), is double integrated in frequency domain to get the curvature displacement $\bar{w}''(x^*,t)$ required for Eq. (8),

$$\bar{w}''(x^*,t) = \mathscr{F}^{-1}\left\{\frac{1}{(\mathrm{i}\,\omega)^2}\,\mathscr{F}\left\{\ddot{\bar{w}}''(x^*,t)\right\}\right\}. \tag{10}$$

However, special care has to be taken when it comes to practical effects like biased or noisy signals as well as unknown initial conditions. A bias at acceleration level only already results in linear drift at velocity and quadratic drift at displacement level. As proposed in [13], drift effects can be minimised by high-pass filtering prior to the integration process. Due to leakage effects, which occur in the DFT and inverse DFT procedure, high-pass filtering is required again after integration in frequency domain. For that reason, a digital high-pass filter with 6^{th} order Butterworth contour according to Fig. 3 was designed.

The entire signal processing within this contribution was performed offline using `Matlab`. By applying reverse filtering methods using the internal `filtfilt` function, the non-linear phase characteristics, see Fig. 3b, could be compensated. However, this procedure is non-causal and therefore generally not applicable to realtime tasks.

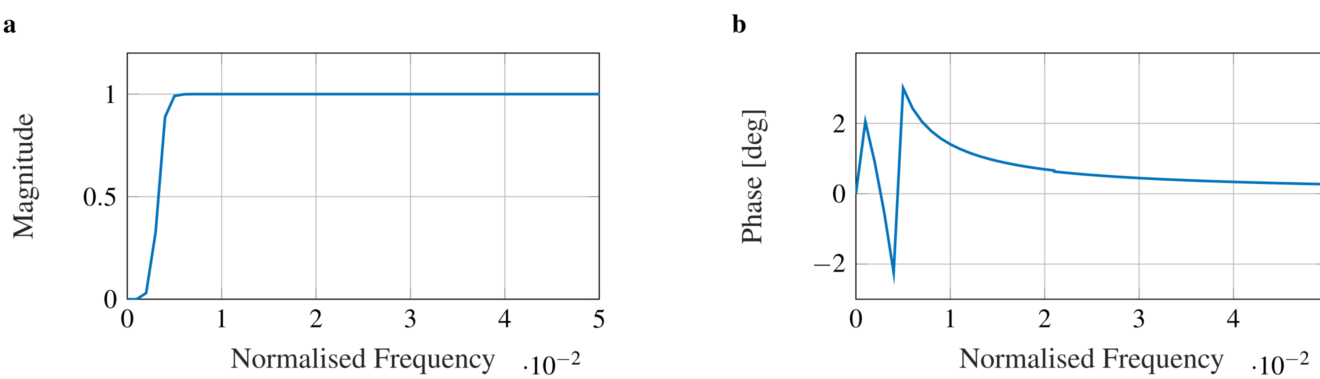

Fig. 3: Frequency response of 6^{th} order Butterworth high-pass filter with $f_{\text{cut}} = 7\,\text{Hz}$; frequency normalised by Nyquist rate $f_N = 2560\,\text{Hz}$. **a** Magnitude plot. **b** Phase plot.

2.3 Fatigue assessment

In order to estimate the actual fatigue progression, structural damage effects have to be derived from strain time histories at critical spots using available damage accumulation models like the widely accepted PALMGREN-MINER rule [14, 15]. According to this hypothesis, fractions of damage are accumulated in linear manner,

$$D = \sum_i \frac{n_i}{N_i}, \tag{11}$$

with n_i being the number of cycles at a stress level σ_i and N_i being the maximal tolerable number of cycles defined by experimental S-N fatigue curves. In order to determine the number of stress cycles n_i, actual stress time histories have to be classified using cycle counting methods, such as rainflow counting [16]. A typical rainflow histogram can be found in Fig. 8d. Structural rupture is generally assumed when D approaches 1.
With readily available strain estimations, Eq. (9), the corresponding uni-axial stress responses can be recovered by taking (e.g. linear) material characteristics into account,

$$\sigma_x(x^*, z, t) \approx \bar{\sigma}_x(x^*, z, t) = E\,\bar{\varepsilon}_x(x^*, z, t), \tag{12}$$

with E being Young's modulus at the considered structural point x^*.

3 Experimental application

After introducing the test setup and suitable quality measures, the MDE principle for the estimation of strains is investigated in two practical test cases with different types of excitation. To evaluate the results in detail, suitable quality measures are introduced.

3.1 Test setup

The investigations within this contribution concentrate on a homogeneous steel cantilever beam structure with properties according to Table 4c. Three `PCB` accelerometers (sensivity: 500 mV/g) were mounted on the surface to observe the first three uni-axial bending modes, Fig. 4b. Reference strains at sensor location x^* were acquired using `Vishay` strain gauges in a full bridge circuit, Fig. 4a. All responses were recorded with a sampling rate of at least 5120 Hz using a `MEDARedSens` data acquisition system. Since the quality of the investigated MDE method strongly depends on the observability of relevant modes, optimal positions x_k, $k = 1, 2, 3$ for the accelerometers were determined using optimisation methods. As proposed in [17], a genetic algorithm was applied.

The computation of optimal sensor positions prior to any measurements is particularly important regarding the future application on more complex structures like a wind turbine. Both sensor installation and the modification of sensor locations is only possible when the turbine is brought to a stop and locked, which is directly linked to economical cuts for the operating company. Thus, standstill periods for installation services must be reduced to a minimum, making available optimal sensor positions fundamental.

3.2 Quality measures

In the two following test cases, strain estimation results $\bar{\varepsilon}_x(x^*, t)$ need to be compared with the corresponding reference time histories $\hat{\varepsilon}_x(x^*, t)$, recorded by strain gauges on the structure surface at location x^*. With $\hat{\epsilon}$ being the sample vector of measured strains during one test period and $\bar{\epsilon}$ being the corresponding sample vector of estimated strains, the Time Response Assurance Criterion (TRAC) [4] can be applied as suitable means,

$$\mathrm{TRAC} = \frac{\left(\bar{\epsilon}^{\mathrm{T}}\,\hat{\epsilon}\right)^2}{\left(\bar{\epsilon}^{\mathrm{T}}\,\bar{\epsilon}\right)\,\left(\hat{\epsilon}^{\mathrm{T}}\,\hat{\epsilon}\right)} \tag{13}$$

a b

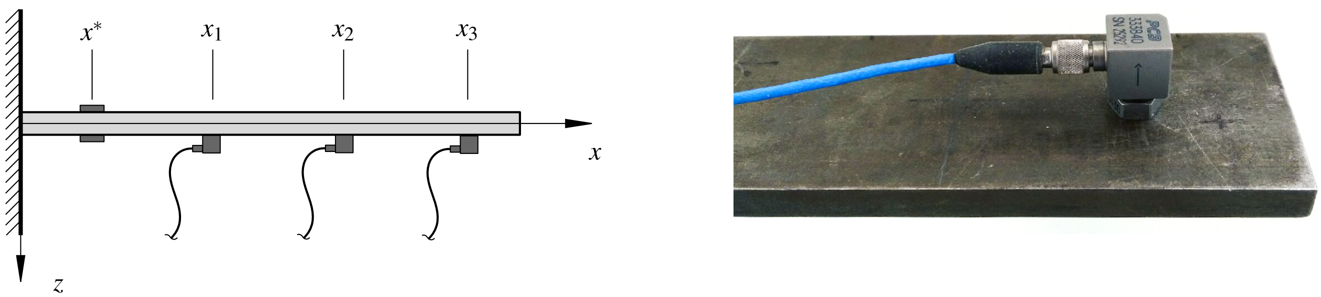

c

Cantilever beam properties			Position	x/ℓ	Sensor type
Young's modulus	E	210 GPa	x^*	0.15	Vishay strain gauges
Density	ρ	7850 kg/m^3	x_1	0.38	PCB accelerometer
Length	ℓ	665 mm	x_2	0.65	PCB accelerometer
Cross section	A	45×8 mm	x_3	0.90	PCB accelerometer

Fig. 4: Experimental setup. **a** Sensor locations on the cantilever beam with accelerometers at positions x_k, $k = 1,2,3$ and strain gauges at position x^*. **b** PCB accelerometer mounted on the beam structure. **c** Experimental setup parameters.

A TRAC value close to 1 indicates a strong correlation between both signals. However, the TRAC is only useful for a qualitative comparison. In order to also account for amplitude differences, the relative error $e(t)$ is introduced,

$$e(t) = \frac{\bar{\varepsilon}_x(x^*,t) - \hat{\varepsilon}_x(x^*,t)}{\max(\hat{\varepsilon}_x(x^*,t))} \tag{14}$$

In Sec. 3.4 a model refinement is conducted on the basis of experimentally obtained modal parameters. In order to measure the correlation between experimentally identified mode shape vectors $\boldsymbol{\phi}_{\mathrm{ex},i}$ and those of the analytical model $\boldsymbol{\phi}_{\mathrm{an},j}$, the Modal Assurance Criterion (MAC) [18] is used,

$$MAC(ij) = \frac{\left(\boldsymbol{\phi}_{\mathrm{ex},i}^{\mathrm{T}}\,\boldsymbol{\phi}_{\mathrm{an},j}\right)^2}{\left(\boldsymbol{\phi}_{\mathrm{ex},i}^{\mathrm{T}}\,\boldsymbol{\phi}_{\mathrm{ex},i}\right)\left(\boldsymbol{\phi}_{\mathrm{an},j}^{\mathrm{T}}\,\boldsymbol{\phi}_{\mathrm{an},j}\right)}, \qquad i,j = 1,\ldots,k, \tag{15}$$

with k being the number of considered mode shapes.

3.3 Free vibrations test

As a first approach, the cantilever beam was statically deflected by an additional mass attached to the free end of the structure by a thin cord. After cutting the connecting cord between mass and beam, i.e. removing of the static load instantly, the beam begins to vibrate according to its eigen-behaviour. The recorded $m = 3$ normalised acceleration responses $\ddot{\boldsymbol{w}}(t)$ at sensor locations x_k, $k = 1,2,3$ are shown in Fig. 5a. After modal decomposition on the basis of analytical mode shapes, estimates for the first $n = 3$ modal accelerations $\ddot{\boldsymbol{q}}(t)$ according to Eq. (6) can be obtained. A section of the corresponding time histories is shown in Fig. 5b. As can be seen, the resulting free vibrations response is mainly determined by the first mode, while $\ddot{q}_2(t)$ and $\ddot{q}_3(t)$ already decay to zero after a short period.

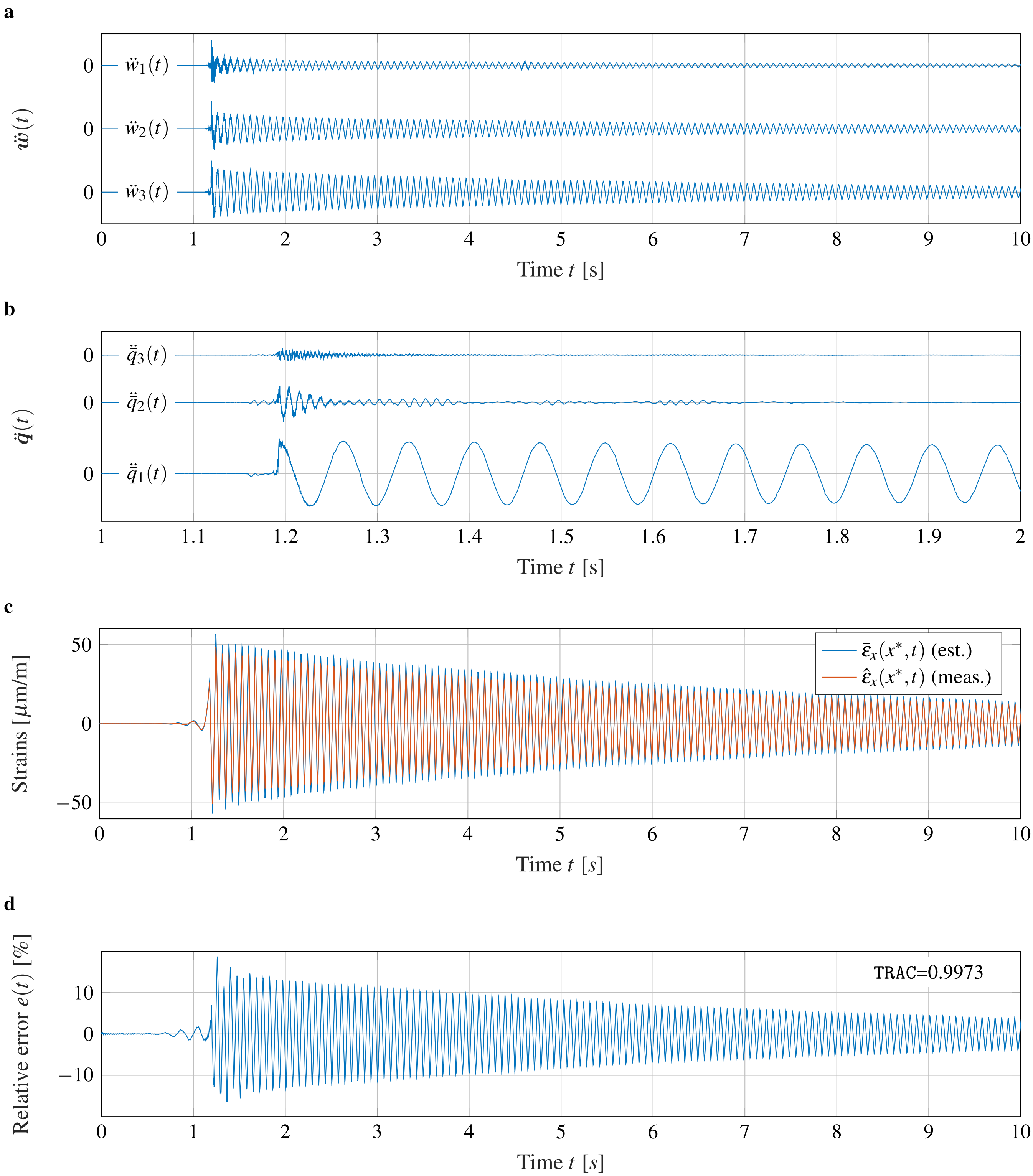

Fig. 5: Results of free vibrations test. **a** Normalised acceleration measurements $\ddot{\boldsymbol{w}}(t)$ at locations x_k, $k = 1,2,3$ **b** Normalised decomposed modal accelerations $\ddot{\boldsymbol{q}}(t)$ **c** Estimated and measured strains at location x^* **d** Relative error $e(t)$

Figure 5c compares the estimated strains $\bar{\varepsilon}_x(x^*,t)$ on the beam surface at location x^* with the corresponding recorded reference strains $\hat{\varepsilon}_x(x^*,t)$. A TRAC value of 0.9973 indicates a very qualitative correlation between both curves. The phase distortion, induced by the high-pass filtering during the double integration process, could be compensated successfully, see Sec. 2.2. However, the strain amplitudes are obviously estimated too high, resulting in a maximal relative error of approximately 15 %, see Fig. 5d.

This exemplary test case demonstrates the general feasibility of strain estimation by using simple analytical mode shapes. Results show a slight amplitude overestimation which, however, is justifiable for conservative fatigue assessments.

3.4 Conclusion from free vibrations test

The previous results indicate that the analytical modal stiffnesses are higher than their actual physical counterparts, resulting from parameter discrepancies between analytical beam model and physical reference structure. As a main influence factor the idealised clamping boundary condition in the model can be identified. The physical clamping undoubtedly exhibits a certain degree of flexibility, which can be additionally considered in the analytical model by replacing the ideal clamping boundary condition with a torsional spring as a first approach.

A reasonable spring stiffness value was determined under the condition that the second eigenfrequency of the physical beam is to be reproduced by the analytical model. Eigenfrequencies and mode shapes of the physical structure were obtained by Experimental Modal Analysis (EMA).

For that approach six acceleration sensors were distributed on the cantilever structure, which was forced to vibrations by an electro-mechanical shaker. A swept sine function with slowly increasing frequency was chosen as excitation signal. One specific frequency response function (FRF) is shown in Fig. 6a, revealing clearly distinct resonant frequencies. The coherence, Fig. 6b, indicates high confidence of the recorded data. Modal parameters were extracted using the least-squares rational function method which is readily available in the `Matlab Signal Processing Toolbox`.

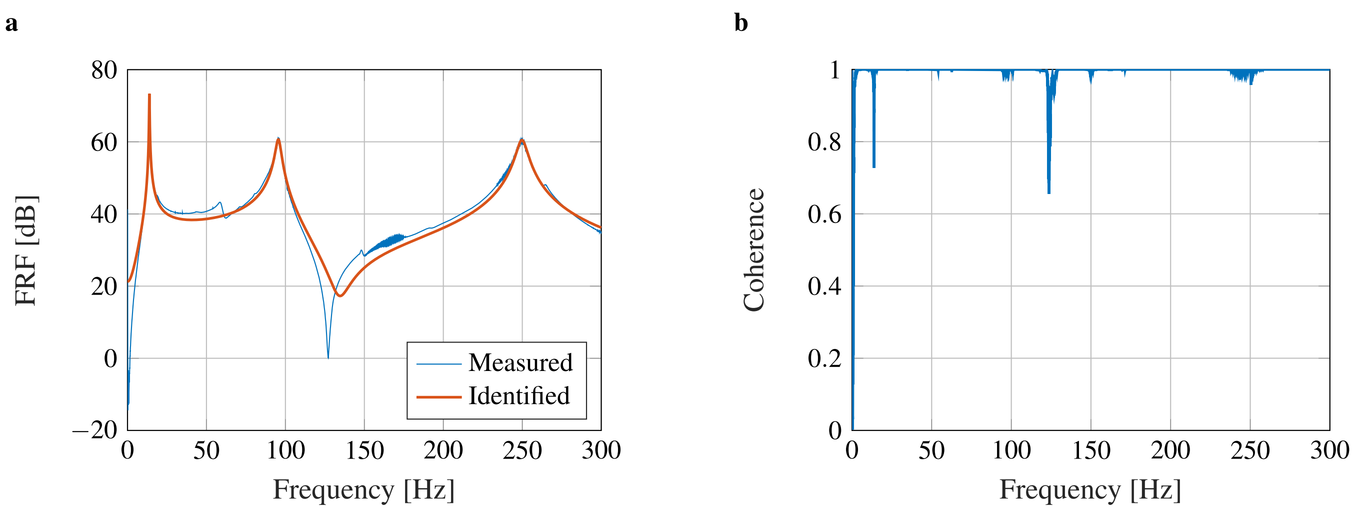

Fig. 6: Selected results of Experimental Modal Analysis. **a** One specific measured FRF and the identified frequency response. **b** Corresponding coherence.

A comparison of the model-based eigenfrequencies and the modal analysis results is given in Fig. 7a. Despite the fact, that the flexible clamping model was adapted to the second eigenfrequency only, also the first and the third eigenfrequencies are reproduced more accurately compared to the model with rigid clamping. Furthermore, the MAC matrix shown in Fig. 7b indicates a high correlation between the experimentally determined mode shapes $\boldsymbol{\phi}_{\text{ex},i}$ and the corresponding analytical mode shapes of the flexible clamping model $\boldsymbol{\phi}_{\text{an},j}$, $i,j=1,2,3$, thus legitimating the flexible clamping approach.

a

Mode	Eigenfrequencies [Hz] Physical structure	Analytical model	Flexible clamping model
1st	14.05	15.11 +7.54 %	14.72 +4.77 %
2nd	92.37	94.72 +2.54 %	92.37 +0.00 %
3rd	247.28	265.23 +7.26 %	258.88 +4.69 %

b

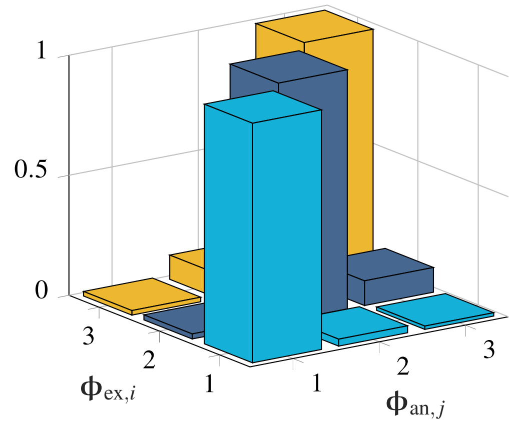

Fig. 7: **a** Experimental and analytical eigenfrequencies **b** MAC matrix of experimental mode shapes $\phi_{ex,i}$ and analytical mode shapes of flexible clamping model $\phi_{an,j}$, $i, j = 1,2,3$

3.5 Forced vibrations test

Since due to the initial conditions mainly first eigenmode vibrations were induced during the free vibrations tests, an additional forced vibrations test was conducted for a larger excitation bandwidth. An electro-magnetic shaker was utilized to excite the structure by a linear frequency sweep up to 300 Hz, i.e. above the third eigenfrequency. In contrast to Sec. 3.3, the MDE was here performed based on analytical mode shapes of the flexible clamping model as derived in Sec. 3.4.

One specific part of the resulting strain responses is presented in Fig. 8a for both measurements and estimations. In order to evaluate possible phase and amplitude differences, Fig. 8b shows an enlarged section of the time histories. Obviously, the amplitude errors could be decreased drastically compared to Sec. 3.3. The corresponding relative error $e(t)$ is reduced to under 5 %, which is already in the range of measurement noise, see Fig. 8c. Larger ringing in the initial phase is due to the settling time characteristics of high-pass filter required in the estimation process. Regarding fatigue estimations, strain or stress time histories, respectively, have to be classified by e.g. rainflow counting methods. For that reason, the rainflow counts of measured and estimated strains are compared in Fig. 8d. After clearing spurious counts due to measurement noise, both spectra show a strong correspondence, resulting in comparable fractions of damage according to Section 2.3.

4 Conclusion & Outlook

In the context of structural dynamics the identification of fatigue indicators at critical spots is of great interest. Within this contribution the widely accepted approach of Modal Expansion and Decomposition is applied in order to estimate axial strains on the basis of a limited number of acceleration measurements. The objective of this contribution is to identify possible pitfalls which are connected with the practical implementation MDE. For this purpose, detailed practical tests were conducted on a steel cantilever beam. As a first approach analytical mode shapes were used for the decomposition and expansion process giving qualitatively meaningful but slightly overestimated strain results. By model refinements based on experimental modal analysis the estimation quality could be increased to a relative error of less than 5 %, which is already at sensor noise level. As a consequence, the estimated rainflow histograms required for fatigue assessment show a good agreement between estimated and measured reference quantities as well.

These results provide a proper basis for future investigations which include the application of this method to physical wind turbines. A suitable basis of relevant mode shapes is available by detailed multibody models which have already been built up and validated for several prototypes [10]. A reasonable model-updating procedure [19] will be conducted on the basis of extensive measurement campaigns on a 3 MW wind turbine.

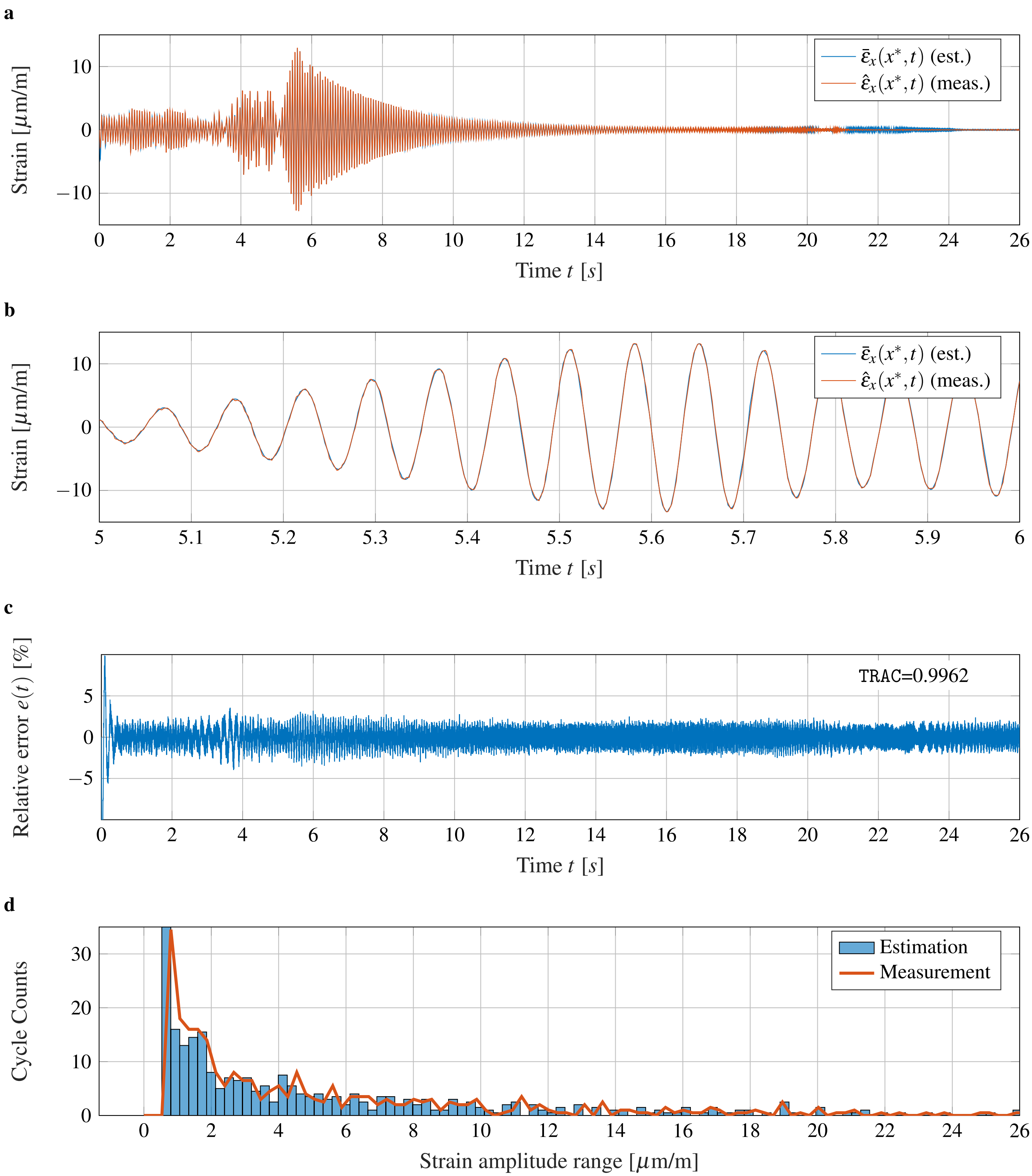

Fig. 8: Results of forced vibrations test under sweep excitation; MDE on basis of beam model with clamping stiffness. **a** Estimated and measured strains at x^* **b** Enlarged section of strain time history **c** Relative error $e(t)$ **d** Rainflow histogram of strain time histories

References

[1] Germanischer Lloyd, "Guideline for the Certification of Wind Turbines."

[2] A. Iliopoulos, W. Weijtjens, D. Van Hemelrijck, and C. Devriendt, "Fatigue assessment of offshore wind turbines on monopile foundations using multi-band modal expansion," *Wind Energy*, vol. 20, no. 8, pp. 1463–1479, 2017.

[3] F. Pelayo, A. Skafte, M. L. Aenlle, and R. Brincker, "Modal Analysis Based Stress Estimation for Structural Elements Subjected to Operational Dynamic Loadings," *Experimental Mechanics*, vol. 55, no. 9, pp. 1791–1802, 2015.

[4] P. Avitabile and P. Pingle, "Prediction of Full Field Dynamic Strain from Limited Sets of Measured Data," *Shock and Vibration*, vol. 19, no. 5, pp. 765–785, 2012.

[5] M. L. Aenlle, L. Hermanns, F. Pelayo, and A. Fraile, "Stress Estimation in a scale Model of a Symmetric Two Story Building," in *5th International Operational Modal Analysis Conference (IOMAC 2013)*, Red Hook, NY: Curran, 2014.

[6] K. Maes, A. Iliopoulos, W. Weijtjens, C. Devriendt, and G. Lombaert, "Dynamic strain estimation for fatigue assessment of an offshore monopile wind turbine using filtering and modal expansion algorithms," *Mechanical Systems and Signal Processing*, vol. 76-77, pp. 592–611, 2016.

[7] R. Rachholz, J. Luthe, A. Schulze, J. Zierath, and C. Woernle, "Development of a dynamically scaled wind turbine," *Journal of Physics: Conference Series (submitted)*, 2018.

[8] J. Zierath, R. Rachholz, S.-E. Rosenow, R. Bockhahn, A. Schulze, and C. Woernle, "Experimental identification of modal parameters of an industrial 2-MW wind turbine," *Wind Energy*, vol. 89, no. Supplement C, p. 260, 2018.

[9] M. Chierichetti, C. Grappasonni, G. Coppotelli, and C. McColl, "A modal approach for dynamic response monitoring from experimental data," *Mechanical Systems and Signal Processing*, vol. 48, no. 1-2, pp. 199–217, 2014.

[10] J. Zierath, R. Rachholz, and C. Woernle, "Field test validation of Flex5, MSC.Adams, alaska/Wind and SIMPACK for load calculations on wind turbines," *Wind Energy*, vol. 19, no. 7, pp. 1201–1222, 2016.

[11] C. Woernle, *Mehrkörpersysteme: Eine Einführung in die Kinematik und Dynamik von Systemen starrer Körper*. Berlin and Heidelberg: Springer Vieweg, 2., erweiterte auflage ed., 2016.

[12] A. Brandt, *Noise and vibration analysis: Signal analysis and experimental procedures*. Chichester, UK: John Wiley and Sons Ltd, 2011.

[13] A. Brandt and R. Brincker, "Integrating time signals in frequency domain – Comparison with time domain integration," *Measurement*, vol. 58, pp. 511–519, 2014.

[14] M. A. Miner, "Cumulative damage in fatigue.," *Journal of Applied Mechanics*, vol. 12, pp. A159–A164, 1945.

[15] A. G. Palmgren, "Die Lebensdauer von Kugellagern," *Zeitschrift des Vereines Deutscher Ingenieure (ZVDI)*, vol. 14, pp. 339–341, 1924.

[16] M. Matsuishi, "Fatigue of metals subjected to varying stress," *Japan Society of Mechanical Engineers*, vol. 68, no. 2, pp. 37–40, 1968.

[17] A. Schulze, J. Zierath, S.-E. Rosenow, R. Bockhahn, R. Rachholz, and C. Woernle, "Optimal sensor placement for modal testing on wind turbines," *Journal of Physics: Conference Series*, vol. 753, p. 072031, 2016.

[18] R. J. Allemang and D. L. Brown, "Correlation Coefficient for modal vector analysis," in *Proceedings of the 1st International Modal Analysis Conference & Exhibit* (Schenectady, N.Y. (1 Union Ave., Schenectady 12308) : Union College, c1982, ed.), pp. 110–116, 1982.

[19] J. E. Mottershead, M. Link, and M. I. Friswell, "The sensitivity method in finite element model updating: A tutorial," *Mechanical Systems and Signal Processing*, vol. 25, no. 7, pp. 2275–2296, 2011.